The Fourteenth International Conference on
Computational Structures Technology
23–25 August, 2022 | Montpellier, France

Proceedings of the Fourteenth International Conference on
Computational Structures Technology
Edited by B.H.V. Topping and J. Kruis
Civil-Comp Conferences, Volume 3, Paper 15.2
Civil-Comp Press, Edinburgh, United Kingdom, 2022, doi: 10.4203/ccc.3.15.2

Pendulum Impact Hammer Tests on Spruce Glued Laminated Timber – Preliminary Results

A.S. Cao, M. Lolli and A. Frangi

Institute of Structural Engineering, ETH Zurich, Switzerland

Abstract

In this paper, preliminary results are presented on pendulum impact hammer tests on full-scale glued laminated timber specimens with dimensions 200x200x3600 mm for the first time. For the tests, a pendulum with an effective mass of 3500 kg and length 4700 mm was built. The pendulum was instrumented with a high-speed camera, angular encoder, optical position-tracking system, and accelerometers. By considering potential energies and the damping in the system, the material toughness was determined to be between 327 and 534 kJ/m2. The maximum impact forces were determined from the deceleration of the pendulum during impact and were between 3565 and 4106 kN. The failure time was determined qualitatively from high-speed imagery to be between 10.18 and 11.58 ms. The dissipated energy is roughly equivalent to the kinetic energy of a 500 kg projectile traveling at 30 km/h.

Keywords: impact loading, GLT, timber, pendulum impact hammer, experiments, disproportionate collapse, structural robustness, tall timber buildings.

1 Introduction

In the 20th century, the use of timber as a structural material has traditionally been restricted to small residential single-family houses. However, timber has seen a surge in popularity as a structural material since the turn of the century. Engineered wood products such as glued laminated timber (GLT), laminated veneer lumber, and cross-laminated timber have been used in several new record-breaking tall timber buildings. These include the current world's tallest timber building Mjøstårnet (85.4 m, 2019) as

well as several planned projects such as the Dutch Mountains (150 & 110 m, 2022-2023).

The current phase of tall timber buildings can be compared with the rise of reinforced concrete structures in the 20th century. It is a phase characterized by rapid innovation through research and practice, often by trial and error. As the volume of timber used in the construction industry is growing at an exponential rate, it is becoming increasingly important to invest sufficient resources into research on robustness and disproportionate collapse prevention in timber buildings to avoid fatal and crippling accidents. Earlier work on robustness and disproportionate collapse in timber buildings include the works of Voulpioutis et al [1], Mpidi Bita et al [2], Huber et al [3], Palma et al [4] and Cao et al [5].

To correctly assess the susceptibility of timber buildings to collapse, state-of-the-art computer simulations are needed. However, data on the failure due to impact for common timber products is practically non-existent. Previous relevant work includes drop-tests on single boards [6–8], pendulum impact hammer tests on 50 to 150 mm square lumber [9,10] and 10 to 20 mm square clear wood [11], and drop hammer tests on guardrails for highways [12]. However, there are difficulties to translate results from previous work to the current engineered wood products used in timber buildings due to the large difference in scale and material.

In this paper, preliminary results from pendulum impact hammer tests on full-scale spruce GLT specimens with 200 mm square cross-sections are shown and discussed. Spruce GLT is currently the most common structural timber material. The effective length of the pendulum is 4.7 m and the mass 3500 kg with a maximum potential energy of about 148 kJ. The pendulum is instrumented with an angular encoder, optical position tracking system, accelerometers, and a high-speed camera operating at 5700 pictures per second.

2 Methods

To assess the failure energy of full-scale engineered wood products, a pendulum was designed and built. The dissipated energy of the specimens during impact can be measured from the difference in potential energy of the pendulum. This is measured by recording the initial and final position of the pendulum and by accounting for the intrinsic system damping. Accelerometers were installed on the pendulum to find maximum impact forces through the deceleration of the pendulum during impact.

The pendulum consists of a 4500 mm HEB-300 beam with steel plates at one end, which purpose is to add mass to the system. At the other end, the HEB-300 beam is connected to a hinge through connector plates. At the hinge-end, an angular encoder is installed to measure the angle of the pendulum. This is the primary measurement device to measure the position of the pendulum and therefore the energy dissipation of the failure. At the tip-end, a high-speed camera capable of 5700 fps is installed facing down in addition to 38400 Hz ADXL1001/2 100/50g accelerometers at the

front end of the hammer. The impact tip is a 300x350x70 mm steel part machined with rounded edges. For redundancy, an optical measurement system using LED-nodes is also installed. A picture of the pendulum is shown in Figure 1.

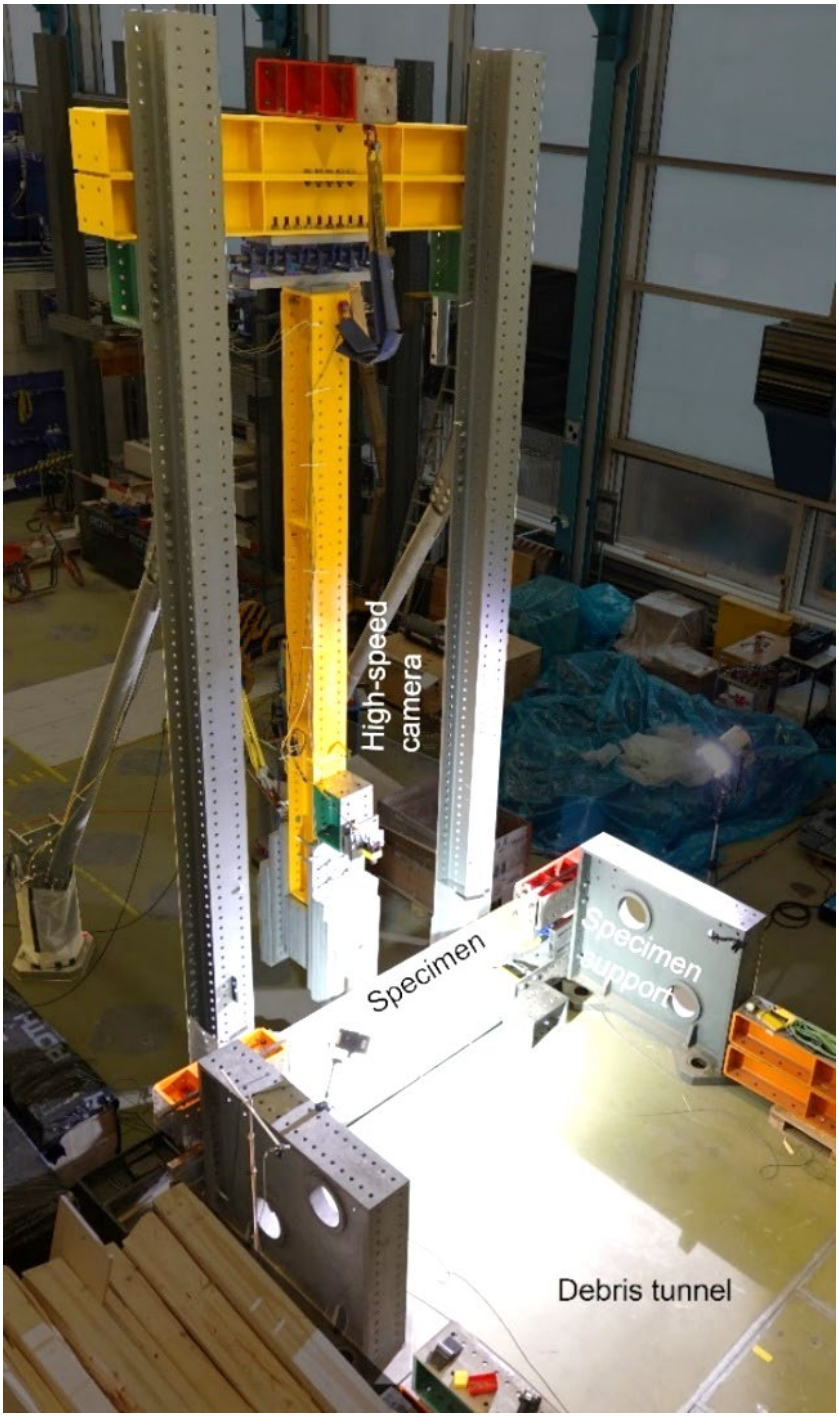

Figure 1: Picture of test setup.

The three specimens have a 200 mm square cross-section and a length of 3600 mm, with the lamellas perpendicular to the pendulum. This is equivalent to a 5-lamella

GLT. Specimens without finger joints were ordered with the density of each lamella noted. For each specimen, the dimensions b, h, l and moisture content ω were measured, as well as the mass m and elastic modulus E_s. The elastic modulus Es was measured from a three-point bending test. The effective length of the specimens for the bending tests were 180 mm shorter than the specimen length. The material properties are summarized in Table 1.

No.	b	h	l	m	ω	E_s	ρ	ρ_l
	[mm]	[mm]	[mm]	[kg]	[%]	[N/mm²]	[kg/m³]	[kg/m³]
200x200x 3600-F-1	199.8	199.8	3602	65.39	11.7	13995	455	437; 433; 434; 437; 483
200x200x 3600-F-2	199.9	199.4	3603	69.19	13.1	13455	482	437; 509; 459; 495; 447
200x200x 3600-F-3	199.5	199.4	3603	72.50	13.2	13597	506	526; 521; 452; 507; 452

Table 1: Material properties of the specimens. The lamella densities ρ_l are listed from the tension side to the compression side.

3 Results

For the three specimens, the maximum impact force F_{max} was between 3564 and 4106 kN. The time from impact to the maximum impact force F_{max} was between 0.55 and 0.57 ms. The time from impact to failure t_f was determined qualitatively as the time from initial contact until each lamella of the specimen developed visible cracks. The failure time t_f was between 10.70 and 11.58 ms. The toughness U_T of the specimens was between 327.12 and 533.51 kJ/m². The results are shown in Table 2.

No.	F_{max}	A_{max}	$t(A_{max})$	$RMS_{max,\ 1\ ms}$	RMS	t_f	ΔE	U_T
	[kN]	×g [m/s²]	[ms]	×g [m/s²]	×g [m/s²]	[ms]	[kJ]	[kJ/m²]
200x200x 3600-F-1	3905.20	115.45	0.55	58.40	34.66	10.70	18.01	451.42
200x200x 3600-F-2	3563.55	105.35	0.52	51.80	35.38	10.18	13.04	327.12
200x200x 3600-F-3	4106.46	121.40	0.57	78.22	47.33	11.58	21.22	533.51

Table 2: Results of the three specimens.

In Figure 2, the absolute value of the acceleration signals |A| and a 1 ms moving $RMS_{1\ ms}$ are shown. By looking closer at the $RMS_{1\ ms}$ in Figure 3, some qualitative observations can be made. At first, the signal increases rapidly upon impact before it reaches a small plateau. This is due to the shock loading of the specimen, where the specimen bounces slightly on the pendulum. Then, the $RMS_{1\ ms}$ reaches its peak before it decreases sharply. Each of the sharp decreases are due to bouncing behaviour, which can be observed from the high-speed imagery. At around the first peak, the outermost lamella develops the first crack. As the trend of the $RMS_{1\ ms}$ decreases, the specimen develops cracks from the tension to the compression side. The different stages of the failure are shown in Figure 4.

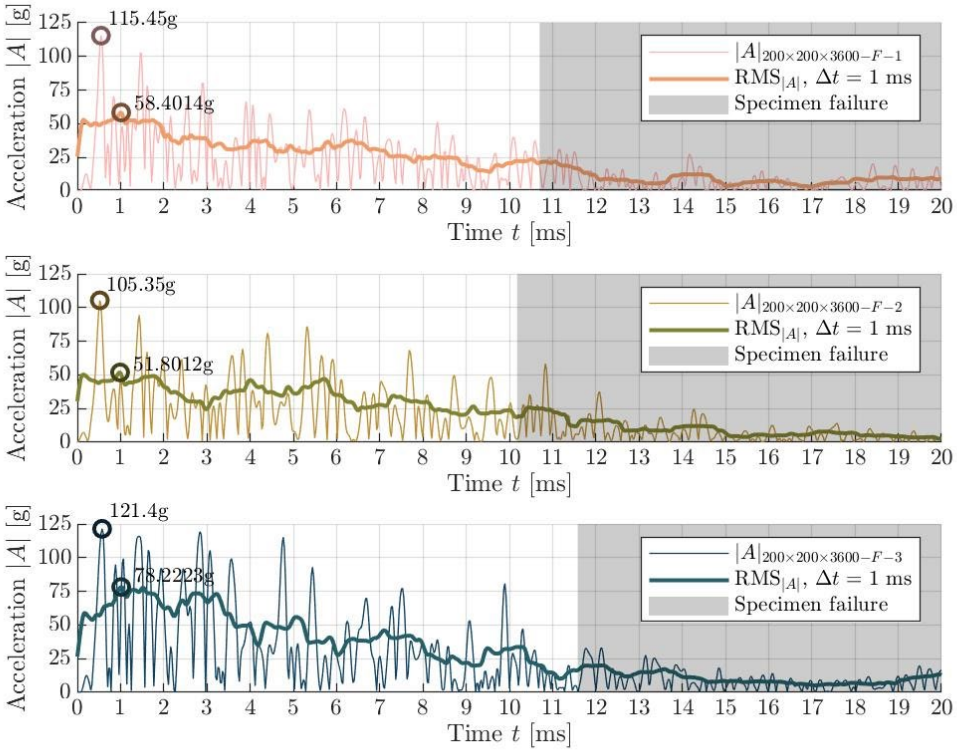

Figure 2: Acceleration signal and moving RMS.

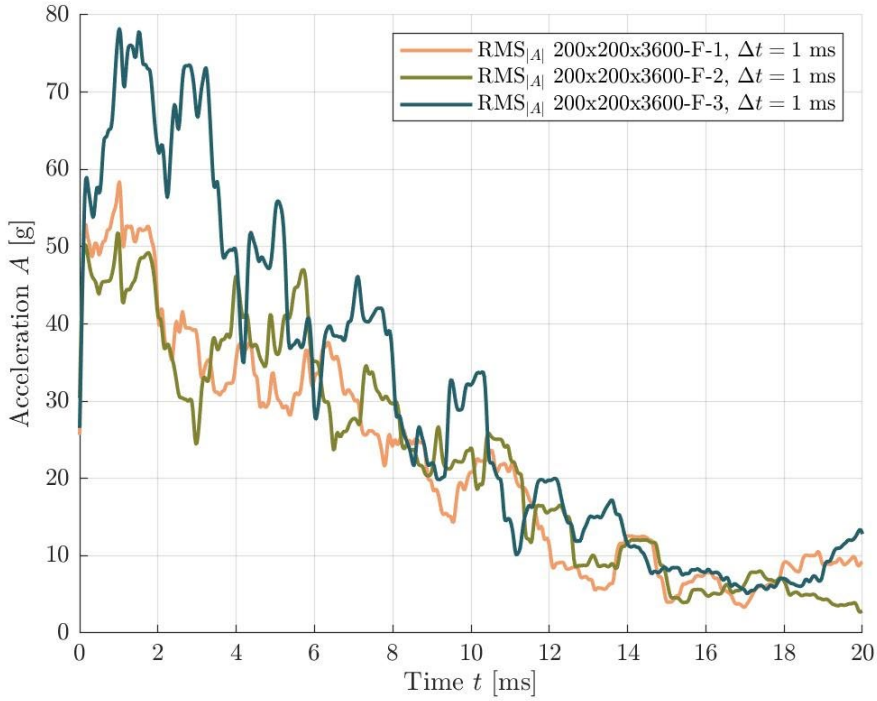

Figure 3: Comparison of the moving RMS.

From the high-speed imagery, several observations can be made about the crack developments. The first failure always occurs at the tension side of the specimen, often near an imperfection such as a knot. This is consistent with the known static properties of the boards, which is weaker in tension than in compression. Then, the failures often propagate from the tension side to the compression side, with a mix of failure modes such as longitudinal shear, tension, and perpendicular shear. This is shown in Figure 4. In some cases, the longitudinal shear failures follow the annual growth rings.

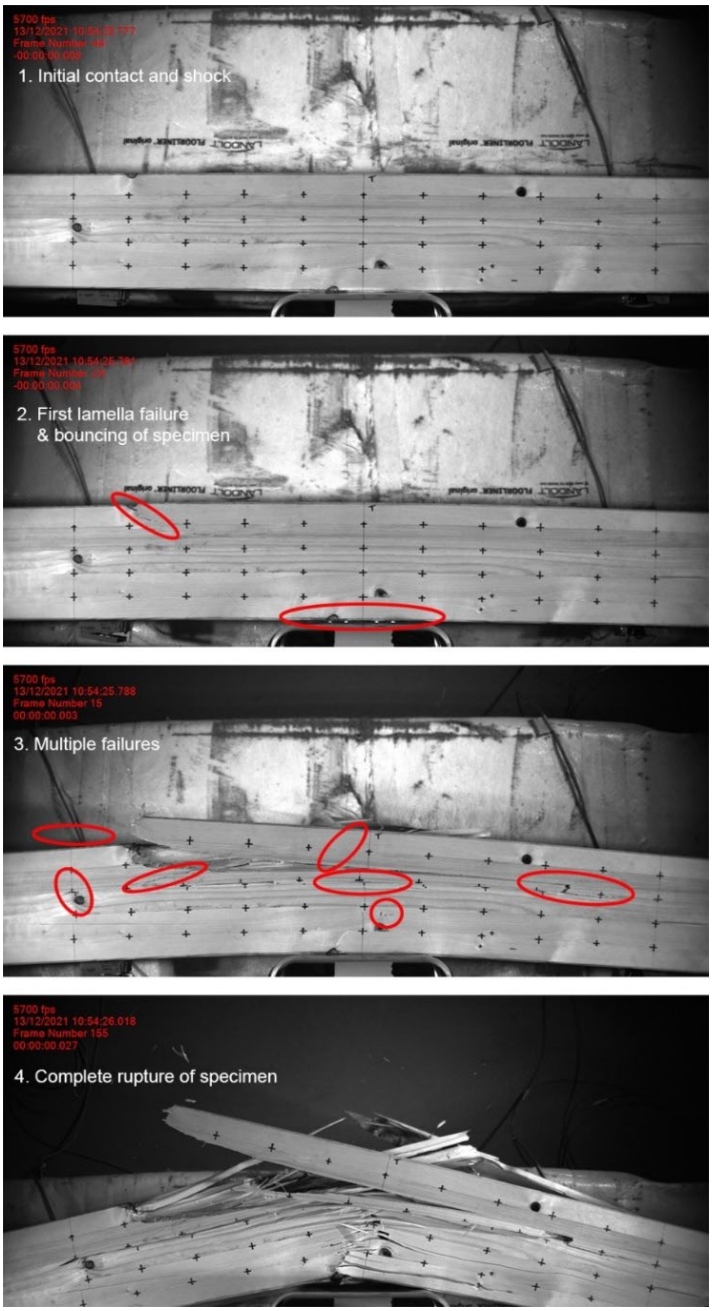

Figure 4: High-speed imagery of 200x200x3600-F-3 during impact.

4 Conclusions and Contributions

In this paper, results from pendulum impact hammer tests on full-scale spruce GLT specimens are shown for the first time. The tests are the first impact tests to be performed on a full-scale engineered wood product and holds great importance to increasing the accuracy of timber building collapse simulations. In turn, this may lead to more robust timber buildings and therefore reducing the risk of disproportionate collapse. In addition, this work contributes to the knowledge on the dynamic response of engineered wood products and may be used to improve and optimize such products.

The pendulum has an effective length of about 4700 mm, initial angle of 85^{o}, and a mass of 3500 kg. The tested specimens were three 5-lamella spruce glued laminated timber specimens with dimensions 200x200x3600 mm. For the three specimens, the maximum impact forces were between 3564 and 4106 kN, time to maximum force between 0.52 and 0.57 ms, failure times between 10.18 and 11.58 ms, and material toughness between 327 and 534 kJ/m^2. The specimens developed cracks from the tension side to the compression side, with a mix of failure modes such as tension, longitudinal shear, and perpendicular shear modes. The cracks were often initiated in regions with visible imperfections such as knots.

The presented results are preliminary results in a larger test regime involving specimens with different cross-sections and length, as well as different boundary conditions. Further tests will be carried out on different engineered wood products such as laminated veneer lumber or cross-laminated timber, and different common wood species.

Contributions

Alex Sixie Cao has contributed to and carried out conceptualization, design, construction, experiments, analysis, and writing of the paper.
Marco Lolli has contributed to and carried out design, construction, and experiments.
Andrea Frangi has contributed to and carried out supervision and proof-reading of the paper.

Acknowledgements

The authors appreciate the assistance and contributions from Roth Burgdorf AG and the Bauhalle team at ETH Zurich.

This article is part of the project *Robustness of tall timber buildings* at ETH Zurich and is funded by the Albert Lück-Stiftung.

References

[1] Voulpiotis K, Köhler J, Jockwer R, Frangi A. A holistic framework for designing for structural robustness in tall timber buildings. Engineering Structures 2021;227:111432. https://doi.org/10.1016/j.engstruct.2020.111432.

[2] Mpidi Bita H, Tannert T. Experimental Study of Disproportionate Collapse Prevention Mechanisms for Mass-Timber Floor Systems. Journal of Structural Engineering 2020;146:04019199. https://doi.org/10.1061/(asce)st.1943-541x.0002485.

[3] Huber JAJ, Ekevad M, Girhammar UA, Berg S. Structural robustness and timber buildings–a review. Wood Material Science and Engineering 2019;14:107–28. https://doi.org/10.1080/17480272.2018.1446052.

[4] Palma P, Jockwer R. Addressing design for robustness in the 2 nd - generation EN 1995 Eurocode 5. International Network on Timber Engineering Research (INTER) - Meeting Fifty-Two, Tacoma (US) 2019:1–22.

[5] Cao AS, Palma P, Frangi A. Column removal analyses of timber structures - Framework to assess dynamic amplification factors for simplified structural design methods. World Conference on Timber Engineering 2021, WCTE 2021, Santiago, Chile: 2021, p. 1717–24.

[6] Leijten AJM. Impact crash and simulation of timber beams. Transactions on Modelling and Simulation, vol. 30, Tallinn, Estonia: 2001, p. 859–68. https://doi.org/10.2495/CMEM010841.

[7] Widmann R, Steiger R. Impact loaded structural timber elements made from Swiss grown Norway spruce. In: Görlacher R, editor. CIB-W18. International council for research and innovation in building and construction. Working commission W18 - timber structures., Karlsruhe, Germany: Universität Karlsruhe; 2009, p. 13–23.

[8] Jansson B. Impact Loading of Timber Beams. The University of British Columbia, 1992. https://doi.org/10.14288/1.0050473.

[9] Pinto Moreira A, da Silveira E, Henrique de Almeida D, Hendrigo de Almeida T, Hallak Panzera T, Luís Christoforo A, et al. Toughness and Impact Strength in Dynamic Bending of Wood as a Function of the Modulus of Elasticity and the Strength in Compression to the Grain. International Journal of Materials Engineering 2017;7:61–7. https://doi.org/10.5923/j.ijme.20170704.01.

[10] Bučar DG, Merhar M. Impact and dynamic bending strength determination of norway spruce by impact pendulum deceleration. BioResources 2015;10:4740–50. https://doi.org/10.15376/biores.10.3.4740-4750.

[11] Baumann G, Brandner R, Müller U, Stadlmann A, Feist F. A Comparative Study on the Temperature Effect of Solid Birch Wood and Solid Beech Wood under Impact Loading. Materials 2021;14. https://doi.org/https://doi.org/10.3390/ma14247616.

[12] Bocchio N, Ronca P, van de Kuilen J-W. Impact loading tests on timber beams. IABSE Conference Report, Lahti, Finland: 2001, p. 349–54. https://doi.org/10.2749/222137801796348818.